# Study on Interfacial Adhesion Strength of Single Glass Fibre/Polypropylene Model Composites by Altering the Nature of the Surface of Sized Glass Fibres

R.-C. Zhuang, T. Burghardt, E. Mäder


# Study on Interfacial Adhesion Strength of Single Glass Fibre/Polypropylene Model Composites by Altering the Nature of the Surface of Sized Glass Fibres

R.-C. Zhuang, T. Burghardt, E. Mäder

PII: S0266-3538(10)00183-1
DOI: 10.1016/j.compscitech.2010.05.009
Reference: CSTE 4714

To appear in: *Composites Science and Technology*

Received Date: 21 December 2009
Revised Date: 3 May 2010
Accepted Date: 5 May 2010

Please cite this article as: Zhuang, R.-C., Burghardt, T., Mäder, E., Study on Interfacial Adhesion Strength of Single Glass Fibre/Polypropylene Model Composites by Altering the Nature of the Surface of Sized Glass Fibres, *Composites Science and Technology* (2010), doi: 10.1016/j.compscitech.2010.05.009

# Study on Interfacial Adhesion Strength of Single Glass Fibre/Polypropylene Model Composites by Altering the Nature of the Surface of Sized Glass Fibres

R.-C. Zhuang[1], T. Burghardt[2], E. Mäder[1*]

[1] Leibniz Institute of Polymer Research Dresden, Hohe Str. 6, 01069 Dresden, Germany

[2] Johns Manville Technical Center, 10100 West Ute Ave., Littleton, CO 80127, U.S.A

[*]Corresponding author. Tel: 49(0)3514658305; Fax: 49(0)3514658362

E-mail address: emaeder@ipfdd.de

**Abstract**

Polypropylene (PP) compatibly sized glass fibres (GFs) were treated with boiling water and toluene, respectively, to reveal the interactions of water and toluene with different components in the sizing of sized GF and their influences on the interfacial adhesion strength of GF/PP model composites. Compared to control GF/PP model composites, about 30% increase of interfacial adhesion strength was achieved for composites with water-treated GF, whereas a small decrease of interfacial adhesion strength was revealed for composites with toluene-treated GF. X-ray photoelectron spectroscopy, Fourier transform infrared spectroscopy, Zeta-potential measurement, and water contact angle measurement demonstrated that the boiling water treated GFs posses a more polar and hydrophilic surface with homogeneously distributed derivatives of γ-aminopropyltriethoxysilane, which is related to a higher interfacial adhesion strength for water treated GF/PP model composites. In contrast, hot toluene treated GFs led to a more hydrophobic surface with low molar mass PP and surfactants enriching on the outermost surface.

**Keywords**: A. Glass fibres, A. Coupling agents, A. Polymer-matrix composites (PMCs), B. Interfacial strength, B. Surface treatments

## Introduction

The interphase between reinforcement GF and matrix in GF/polymer composites is of vital importance since the mechanical properties of composite materials are mainly determined by

whether the mechanical stresses can be efficiently transferred from matrix to the reinforcing fibres[1-4]. It is established that the interfacial properties of composites are mainly determined by the reactivity and compatibility between the matrix composition and the surface properties of used GFs. Tailoring the nature of the GF surface, e.g. chemical composition or geometry, has long been used to enhance GF-matrix adhesion by increasing the covalent bond density, mechanical interlock, etc [5]. From the industrial production point of view, on-line coating as-spun GF with an appropriate sizing is the most straightforward means to meet this objective [6].Usually, a sizing is an aqueous mixture of polymeric film former, coupling agent, processing aids (such as lubricant) and/or other additives [7, 8]. In general, the good combination of sizing components plays an important role in determining the GF-matrix adhesion [9].

It is noted that under aqueous condition the functional groups, mostly amino group, of (hydrolyzed and condensed) silanes and the polar groups of surfactants and additives are able to interact with the surface silanol group of the GF via H-bonding, electrostatic interaction or dipole-dipole interaction [10-14]. Meanwhile, the physically adsorbed polysiloxanes may degrade the GF-matrix adhesion [15]. As a result, the fracture of GF reinforced composites usually initiates at weak areas in the interphase, e.g. with low coupling agent density, and then progresses through the matrix. Great efforts have been conducted to understand the influence of these weak aspects [3, 5, 16-19]. Among them, treating sized GFs with solvents, usually acetone or water, to partly wash out unwanted components is a simple way for fundamental research. Prior works in this field mainly focused on GFs sized with pure silane coupling agents [3], only a few studies were performed on GFs sized with the complete sizing package and most of them were conducted on thermosetting polymer compatible GFs[18-22]. There are limited studies on PP compatibly sized GFs. In this study, water and toluene were used to selectively extract a PP compatible GF.

Extracting GF with hot water is similar to aging. The aging of sizings was already investigated by Ishida and Koenig in 1979 [23], the significant changes on silane treated E-glass surface after

storage in water at 80 °C were observed. However, they did not correlate the surface changes with the adhesion strength changes in composites. Jones et al. extracted 1% 3-aminopropyltriethoxysilane (γ-APS) sized GF with 40 °C warm water and 100 °C hot water sequentially and confirmed that the sizing layer structure is the same as the reported one [21, 24, 25]. Moreover, it was found that adsorbed water molecules could migrate towards the sizing/GF interface through the thin sizing, resulting in the dissolution/decomposition of polysiloxane [15, 26] or the growth of a silica gel layer [27]. On the other hand, it is known that surfactant adsorbed on glass plates can be replaced with polymer solution or washed away by solvents, even though Jones et al. found that solvent extraction could not remove sizing resins efficiently [28, 29]. Recently, it was revealed by Mäder et al. that extracting only γ-APS sized GFs with hot water led to a great increase in the local interfacial shear strength and the energy release rate of epoxy/GF single fibre model composite since water washed off excessive physically adsorbed γ-APS [16]. The same effect was also observed by Jones et al. in their studies on AR glass and E-glass reinforced vinyl ester composites [19]. Hence, it is worthwhile to know the interaction of water molecules with PP compatibly sized GF and the influence of the surface change on the properties of the resulting model composite.

At elevated temperature, toluene is a good solvent for PP, polymeric film former of PP compatible sizings, and the physically adsorbed polysiloxane [30]. Therefore, extracting sized GF with hot toluene can remove the physically adsorbed polysiloxane, the low molecular weight (MW) fraction of PP[31], and surfactants. On the other hand, long time exposure to hot toluene can also lead to the enrichment of hydrophobic PP, especially the small MW fraction of PP [32], on the outermost surface of sizing layer due to solvent annealing effect, this might lead to a more ductile or a weaker interphase.

In this work, surface sensitive analysis methods (dynamic contact angle measurement, atomic force microscopy (AFM), X-ray photoelectron spectroscopy (XPS), and Zeta-potential measurement)

were used to probe the changes of surface properties of as-spun and differently treated GFs. The influence of hot water and toluene treatments on the interfacial adhesion strength of single fibre/PP model composite was studied using single fibre pull-out test.

**Experimental Details**

**Materials.** Toluene (Acros) and γ-APS (Degussa) were used as received. Water was deionized to a resistivity of 15 MΩ·cm using a Millipore Elix 5 water purification system. E-glass fibres sized by γ-APS in conjunction with PP film former (about 1:2.6 in dry weight ratio) were spun at the Leibniz Institute of Polymer Research Dresden using a continuous spinning device comparable to industrial ones. The average diameter of used sized GF is 15 μm. The as-prepared sized GF is named M1. M1 was extracted with boiling water and toluene for 8 h using a Soxhlet extractor with the aim to selectively extract sizing layer, the resulting GFs are referred as M1-W and M1-T (shown in Tab. 1), respectively. An isotactic polypropylene (weight average molecular weight ($M_w$) = $23.8 \times 10^4$ g/mol) compounded with 2 wt.% MAH-g-PP (Polybond 3200) was used as matrix.

**Methods.**

High temperature gel permeation chromatography (HT-GPC) was performed at 150 $^oC$ using trichlorobenzene as solvent and eluent on a PL GPC220 (Polymer Laboratories) equipped with 2 PL Mixed B LS separating columns using triple detection (refractive index, light scattering, and viscosity). Room temperature GPC was carried out on a PL GPC220 (Polymer Laboratories) equipped with a PL Mixed-C column using tetrahydrofurane as solvent and eluent.
XPS investigations were performed on a Kratos AXIS Ultra X-ray photoelectron spectrometer. Areas of approximately 300 x 700 microns were analyzed with a monochromatic Al Kα X-ray source. The samples were analyzed via angle-resolved XPS (AR-XPS) at normal (90º) and glancing (60º, 30º, and 15º) take-off angles (TOAs) in order to investigate the sizing surface chemistry as a function of analysis depth. The TOA is the angle between the analyzer and sample surface. At a 90º TOA, the XPS is capable of analyzing the top 8 nm of the sample surface, while at a 15º TOA only the top 2-2.5 nm of the sample surface is investigated. Due to the insulating nature of the samples, charge neutralization of the sample surface was required. Survey spectra were collected from six different areas of each sample at 90º TOA and 2 areas of each sample at 60º, 30º, and 15º TOAs.

The survey spectra were collected over a wide binding energy range (0-1300 eV) and were used to evaluate all of the elements present (except H and He) within the sample surface. The survey spectra were acquired at a pass energy of 160 eV and a step size of 1 eV. The high-resolution spectra were dissected by means of the spectra deconvolution software. The parameters of the component peaks were their binding energy, height, full width at half maximum, and the Gaussian-Lorentzian ratio.

Tapping mode AFM measurements were carried out using Dimension 3100 (Digital Instruments, Santa Barbara) at room temperature. The values of root-mean-square roughness ($R_q$) and maximum height roughness ($R_{max}$) were calculated over the AFM images (3 µm x 3 µm).

Electrokinetic properties, Zeta-potential as a function of pH, of sized GFs were obtained by electrokinetic analysis (EKA) on an electrokinetic analyzer (Fa. Anton Paar KG, Austria).

The dynamic advancing contact angle ($\theta_a$) and receding contact angle ($\theta_r$) measurements on single GFs were performed on a tensiometer K14 (Krüss GmbH, Hamburg, Germany).

The FTIR investigations were carried out on a Bruker IFS66 spectrometer. Transparent polymer films of PP film former and its acetone insoluble part with a thickness of 250 µm were prepared by compression molding at 190 $^{o}$C. All extractions were analyzed in form of KBr pellets.

The NMR spectra were collected on a Bruker DRX 500 NMR spectrometer at 500.13 MHz for $^{1}$H NMR spectrum and 125.75 MHz for $^{13}$C NMR spectrum. The signal assignment was done by $^{1}$H-$^{1}$H COSY and $^{1}$H-$^{13}$C HMQC 2D NMR experiments using the standard pulse sequences provided by Bruker. For internal calibration the solvent peaks of DMSO-$d_6$ were used: $\delta$ ($^{13}$C) = 39.60 ppm; $\delta$ ($^{1}$H) = 2.50 ppm. $^{13}$C NMR spectrum was used for peak assignment and is not shown at here.

Single fibre pull-out test was performed on single fibre model composites to study the interfacial adhesion strength. The fibres were end-embedded 300 µm deep into matrix at 200 $^{o}$C with a heating and cooling rate of 50 K/min. From each force-displacement curve, the force $F_d$ at the start of debonding and the embedded length, $l_e$, were derived. The apparent adhesion strength $\tau_{app}$ was

determined according to eq. 1

$$\tau_{app} = \frac{F_d}{\pi D_f l_e}, \quad (1)$$

where $D_f$ is fibre diameter.

The local adhesion strength $\tau_d$ and the critical interphase release rate $G_{ic}$ were calculated according to

$$\tau_d = \pi(D_f/2)^2[-p + (p^2 - q(G_{ic})^{1/2}] \quad (2)$$

where $p$ and $q(G_{ic})$ are terms depending on fibre and matrix properties and specimen geometry [33].

**Results and discussion**

**Remarks on M1 fibre and used PP film former**

The organic content of M1 fibre is 1.1 wt.% determined by pyrolysis following DIN EN ISO 1172. The average sizing thickness is about 36 nm assuming a homogenous sizing was formed and the density of sizing is 1 g/cm$^3$. The commercially available PP film former is in the form of aqueous dispersion with a solid content of 35 wt.%, which was added drop-wise to acetone to get an acetone soluble part (Part-I) and an acetone insoluble part (Part-II), the weight ratio of Part-II to Part-I is about 4:1. Part-I was subjected to NMR, FTIR, and GPC analyses while Part-II was analyzed using FTIR and HT-GPC. The results are shown in Fig. 1 and Fig. 2 for $^1$H NMR spectrum and FTIR spectra, respectively. The NMR spectrum of Part-I (Fig. 1) revealed that the main fraction of Part-I is alkyl polyethylene glycol ether. The peak assignment is detailed in following. The triplet peaks centered at 0.85 ppm are assigned to the $CH_3$- of alkyl group. The intensive peak at 1.24 ppm arises from the -$CH_2$- of alkyl group. A group of multiplet peaks between 3.3~3.6 ppm, except the resonance peak of $H_2O$ at 3.51 ppm, are due to the resonance of -$CH_2O$-. Additionally, Part-I has a small amount of low molecular amines, most likely *N*-methyl ethylamine and/or its derivatives. The singlet peak at 2.37 mainly arises from the $CH_3N$- of *N*-methyl ethylamine, while the quadruplet

peaks between 2.76~2.80 are attributed to the resonance peak of -$CH_2$N- of *N*-methyl ethylamine next to methyl group, which gives raise to the triplet peaks around 1.06 ppm. On the other hand, the FTIR spectrum of Part-I (Fig. 2d) shows only the typical absorbance bands of alkyl polyethylene glycol ether. In detail, the strong absorbance bands between 1080~1150 $cm^{-1}$ are attributed to the stretching vibration of C-O, the intensive band at 1464 $cm^{-1}$ arises from the bending vibration of $CH_2$, while the broad band between 3200~3600 is assigned to the stretching vibration of OH and/or NH. GPC analysis revealed that the number average molecular weight (Mn) of Part-I is 920 g/mol with a narrow polydispersity index of 1.25. The main component of Part-II is MAH-*g*-PP, as revealed by FTIR in Fig. 2e. Except the typical absorbance bands of isotactic-PP, additional bands at 1775 and 1735 $cm^{-1}$ are attributed to the stretching vibration of anhydride and other carbonyl groups. HT-GPC showed that Part-II has Mn of 75400 g/mol, which is quite close to that of PP dispersion (80600 g/mol). Moreover, Part-II has also a tiny amount of surfactant or other low MW components, as a weak peak at low molar mass region was present in the HT-GPC curve.

**Analyses on extractions**

Extracting M1 fibre in hot water and toluene, respectively, both led to a weight loss, the weight loss of M1 fibre is slightly higher in the case of hot water treatment (Tab. 1). It is noted that both hot water and toluene extracted mainly one component from the sizing layer, basing on the following observations. The extract in hot water was subjected to FTIR analysis and the result is shown in Fig. 2a. For a better comparison, Fig. 2c and Fig. 2b show the FTIR spectra of acetone soluble part of PP dispersion and the extract of only γ-APS sized GF using hot water, respectively. For the extract of only γ-APS sized GF (Fig. 2b), the absorbance bands at 2923 and 2852 $cm^{-1}$ are assigned to asymmetric and symmetric stretching vibration of >$CH_2$, the strong and broad peak at 1029 $cm^{-1}$ is the typical stretching absorbance band of Si-O-Si. The absorbance bands between 1650~1130 $cm^{-1}$ are attributed to the stretching vibration of carbonyl group and bicarbonate salts due to the interaction between the amino group of γ-APS based components and environmental $CO_2$ and water

[34,35]. From the similarity between Fig. 2a and Fig. 2b one can conclude that the wash-out of M1 fibre in hot water mainly is γ-APS based components. Since the intensity of the peaks at 2923 and 2852 $cm^{-1}$ is stronger in Fig. 2a, alkyl polyethylene glycol ether could be also included. However, the wash-out might also comprise small molecular amines and small amounts of PP, which bond or interact with physically adsorbed γ-APS based components and were extracted into water with physically adsorbed γ-APS based components.

Upon extraction in hot toluene, mainly alkyl polyethylene glycol ether was washed out as revealed in the FTIR spectrum (Fig. 2d). However, components with Mn of 23800 g/mol were detected by HT-GPC, this fraction can be assigned to PP or the complex of PP with γ-APS, since it is known that the physically adsorbed γ-APS based components do not posses such high MW [25]. Nevertheless, one can not exclude the presence of this part, its concentration might be just beyond the sensitivity of methods used.

**Surface properties of fibres**

The impact of solvent treatment on the surface properties of GFs was firstly studied by mapping the surface topography using tapping mode AFM. Fig. 3 presents AFM height images of M1-T and M1-W fibres as well as M1 fibre, the surface roughness data of GFs are summarized in Tab. 1. Fig. 3a shows that the surface of M1 fibre looks like pine tree bark characterized by the irregular islands in a sea. Upon extraction with hot toluene, the surface of M1-T fibre turns rougher (Fig. 3b), which probably is due to the swelling of toluene in sizing during extraction, which collapsed or shrank in the course of drying at 80 $^{o}$C under vacuum. Correspondingly, the $R_q$ and $R_{max}$ values increase from 3.5 and 41.5 nm to 9.6 and 88.6 nm, respectively. On the other hand, extracting M1 fibre in hot water did not change the surface topography of the resulting fibres as much as in hot toluene. There is only a small increase in both $R_q$ and $R_{max}$ values.

Water contact angle measurements were performed to obtain information concerning the hydrophobicity of the sizing of single fibres. Tab. 1 summarizes dynamic advancing contact angles

($\theta_a$) and receding contact angles ($\theta_r$) as well as the hysteresis value ($\theta_a$ -$\theta_r$). The control M1 fibre has $\theta_a$ of 94.3$^o$ and $\theta_r$ of 68.5$^o$. After toluene extraction, $\theta_a$ and $\theta_r$ of M1-T fibre increase a little bit to 99.2$^o$ and 72$^o$, respectively. As FTIR and HT-GPC analyses revealed that surfactants and PP with low MW were extracted into hot toluene, the higher water contact angle is related to the enrichment of low MW PP on the topmost surface since PP with lower MW has lower surface tension compared to the high MW analogues [32]. Extracting M1 fibre with boiling water altered the surface of sized GF from hydrophobic to hydrophilic, indicated by the significant decrease of both $\theta_a$ and $\theta_r$. This could be due to two reasons. One is that amide groups, imide groups and/or ester groups converted into more hydrophilic carboxyl groups via hydrolysis reaction, meanwhile the polysiloxane also underwent hydrolysis resulting in more polar silanol groups. This is confirmed by XPS analysis demonstrated in next paragraphs. The other reason is the annealing affect, the high temperature and highly humid atmosphere drove polar groups to migrate towards the sizing/air interface.

AR-XPS was used to probe the radial distribution of sizing components within the sizing, the average surface compositions in atomic percentage are presented in Tab. 2. The C 1s high resolution spectra were curve-fitted with four peaks. The corresponding peak assignments are listed in Tab. 3. The peaks of interest in the C 1s spectra are C-1 and C-2, which correspond to C-C and C-N/C-O chemical states, respectively. C-3 and C-4 correspond to different types of surface oxidation of the carbon. In addition, the N 1s high resolution spectra were curve-fitted with two peaks, which correspond to amine and protonated amine chemical states. Here, only the degrees of nitrogen protonation are reported in Tab. 3.

For the M1 fibre, a 20% increase in C and 40% decrease in N were found at 15$^o$ TOA versus at 90$^o$ TOA, while the percentage of C-C bonds remained constant and there was a 10% decrease in C-N/C-O bonds. This agrees with the results of contact angle measurements indicating the non-polar components of polymeric film former enrich on the outermost surface. In addition, it was determined that at 90$^o$ TOA 10% of the amine groups are protonated while no protonation was

observed at the air/sizing interface. Usually it is assumed that the protonation of the amino group is mostly induced by the interaction of amino groups with silanol groups either via intra-molecule or inter-molecule H-bondings [10-14]. Thus a higher degree of protonation serves as indirect evidence supporting the above observation that the aminosilane is enriched at glass/sizing interface.

For the toluene washed fibre (M1-T), at TOA of 90°, a 5% decrease in C was detected while the N percentage was similar to the M1 fibre. This small drop in C correlates to the FTIR and GPC results, which revealed surfactants and PP in the toluene extract. In addition, a 30% increment in C and 35% decrease in N were observed at 15° TOA in comparison with at 90° TOA. These results are similar to those found for the M1 fibre prior to extraction. Moreover, C-C bonds show about a 10% increase while about 40% reduction in C-N/C-O bonds was found compared to the M1 sample, which is in a good agreement with the FTIR analysis of the wash-off of M1 fibre in hot toluene. On the other hand, a 5% drop in C-C bonds and about 30% increment in C-N/C-O bonds were observed as the TOA was decreased. The large increase in the C-2 peak is probably due to an enrichment of the C-O bonds from either polyethylene glycol or oxidation of the outermost surface of the fibre or more amino groups are present in the outermost surface upon extraction as observed by Zeta-potential measurement. Moreover, it was found that 20% of the amine groups at TOA of 90° are protonated while no protonation was found at the outermost surface of the fibre.

For the water washed fibre (M1-W), at TOA of 90°, a 15% drop in C and 40% decrease in N were observed compared with the M1 sample. A 10% increase in C-C bonds and 30% decrease in C-N/C-O bonds were observed compared to the M1 sample. This suggests that the boiling water extraction removed physically adsorbed and/or chemisorbed coupling agent and surfactants from sizing and consists with the FTIR analysis on the wash-off of M1 fibre using hot water.

Furthermore, a 12% reduction in C was detected at TOA of 15° versus at TOA of 90°, while the N percentage remained constant as a function of probing depth. In addition, it was observed that almost 50% of the amine groups at TOA of 90° have been protonated, while 35% are protonated at the outermost surface. This agrees with the contact angle observation that the polar groups are

present on the outermost surface, thus creating a hydrophilic surface. On the other hand, the C-1 and C-2 percentages remained constant as a function of depth probed into the surface. This suggests that the concentration of aminosilane does not change greatly within the detected information depth. To better understand the influence of solvent treatments on the surface properties of GFs, Zeta-potential of GF was determined using EKA to derive information about the surface functional groups. The Zeta-potential ~ pH curves are shown in Fig. 4. Compared with M1 fibre, a significant shift in iso-electric point (IEP) to the basic region after toluene treatment or to the acidic region after water treatment was found. After toluene treatment a significant amount of surfactant and a part of the PP film former were removed. As a consequence, the basic $NH_2$-groups of the aminosilane are more accessible, correspondingly the Zeta-potential at the plateau shifted to higher positive values, meanwhile the IEP also moved from 7.0 to more basic value. On the contrary, after water treatment the Zeta-potential of M1-W fibre at native pH shifted from positive to negative and preferably acidic groups were detected at the surface, moreover the IEP was shifted to about pH 4. These results also suggest the hydrolysis of siloxane groups and migration of aminosilane from sizing/fibre interface to air/sizing interface.

From above analyses the radial chemical compositions of GF sizing layer become clear and are presented in following. After sizing application and drying, the sizing of control fibre (M1) shows enrichment of aminosilane in the sizing/GF interface while PP film former predominating at the air/sizing interface. The driving force for this is related to the low surface free energy of PP and the good affinity between aminosilane and GF surface. Upon extraction in hot toluene, the low MW fraction of PP film former and surfactants are partly washed off, making the amino groups of aminosilane more accessible; however, the low MW PP and surfactants enrich on the outermost surface. Extracting sized GF in hot water can wash off physically adsorbed and chemisorbed aminosilane and surfactants. Under high humidity and high temperature, polysiloxane hydrolyzes and distributes evenly throughout the detected information depth. Moreover, hot water extraction led to GF with a more hydrophilic surface.

**Single fibre pull-out test**

Interfacial shear strength is an evaluation of the efficiency of the interface to transfer the applied stress from the matrix to the fibre before interfacial debonding occurs. In-house single fibre pull-out test device was used to determine the interfacial adhesion strength of differently treated GF/PP model composites. Tab. 1 shows a modest decrease of the local adhesion strength $\tau_d$ and $G_{ic}$ when M1 fibre was extracted in toluene, the $\tau_d$ and $G_{ic}$ slightly drop from 13.1 MPa and 5.5 J·m$^{-2}$ to 10.6 MPa and 3.7 J·m$^{-2}$, respectively. Based on the results of Zeta-potential measurement this was not expected, since it revealed a better accessibility of the amino groups of aminosilane, which can prompt the formation of the covalent bond between amino group and anhydride group. However, if the enrichment of low MW PP and surfactants at the outermost surface is taken into consideration, the modest drop in interfacial adhesion strength is reasonable and could relate to the presence of weak points in the interphase. This is consistent with our previous observation that the bond strength was especially low when low MW PP was applied as film former [31]. On the other hand, water extraction removed a part of the silane coupling agent, which is physisorbed on the GF surface, and small molecule surfactants. Additionally, the interpenetrating network of polymeric film former and aminosilane caused by the hot water extraction enhances the inter-diffusion of sizing and matrix promoting the formation of covalent bonds between amino groups and anhydride groups. In this case, the local adhesion strength $\tau_d$ and the critical interface energy release rate $G_{ic}$ are significantly increased up to 21.0 MPa and 14.7 J·m$^{-2}$, respectively.

**Conclusion**

PP compatibly sized glass fibres (GFs) were subjected to extraction either in hot water or in toluene to simulate a different attack of sizing depending on the media and in depth altering of the sizing, respectively, and to obtain indirect information about the gradient within the interphase ranging from the air/sizing interface to the sizing/glass interface. FTIR and GPC anaylses on the wash-offs, surface properties of GFs and the interfacial adhesion strength of single fibre/PP model composites

upon extraction in different liquids proved to be surface sensitive methods, revealing the chemical composition within the sizing. Extracting control GF in hot toluene, surfactants and the low molecular weight fraction of PP film former are partly washed off, making the amino groups of aminosilane more accessible; however, the enrichment of low molecular weight PP and surfactants on the outermost surface creates weak points in the interphase. The latter one overwhelms the former one leading to slight decrease in interfacial adhesion strength. On the other hand, extracting control GF in hot water could wash off physically adsorbed and chemisorbed aminosilane and surfactant. Meanwhile polysiloxane hydrolyzes and distributes evenly throughout the sizing thickness, as a result of this the observed interfacial adhesion strength value shows a 30% increase. Further works will be dedicated to Nano-indentation and Nano-TA studies on differently treated GFs and corresponding composites to evaluate the mechanical property and chemical composition gradient within sizing/interphase thickness with the aim to deepen the understanding on the correlation between the surface/interphase properties and composite material mechanical properties.

**Acknowledgements**

RCZ would like to thank Johns Manville and Leibniz Institute of Polymer Research Dresden for funding the stay as postdoc. The authors are indebted to Mrs. G. Adam, Dr. C. Bellmann, Dr. H. Brodowsky, Mrs. R. Plonka, Mr. J. Rausch, Mrs. A. Rothe, Mrs. P. Treppe (IPF Dresden e.V), Dr. J. Asrar, Dr. D. Blasini, Dr. A. Ferryman, and Dr. K. Gleich (JMTC) for their experimental assistance and helpful interpretations.

**References**

[1] Kim JK, Mai YW. High strength, high fracture toughness fibre composites with interface control-A review. Compos. Sci. Technol. 1991;41(4):333-78.

[2] Pukánszky B. Interfaces and interphases in multicomponent materials: past, present, future. Eur. Polym. J. 2005;41(4):645-62.

[3] Ishida H. A review of recent progress in the studies of molecular and microstructure of coupling agents and their functions in composites, coatings and adhesive joints. Polym. Compos. 1984;5(2):101-23.

[4] Mäder E, Pisanova E. Interfacial design in fiber reinforced polymers. Macromol. Symp. 2001;163:189-212.

[5] Jones FR. Interphase formation and control in fibre composite materials. Key. Eng. Mater. 1996;116-117:41-60.

[6] Thomason JL, Adzima LJ. Sizing up the interphase: an insider's guide to the science of sizing. Compos. A: Appl. Sci. Manufact. 2001;32(3-4):313-21.

[7] Frenzel H, Bunzel U, Häbler R, Pompe G. Influence of different glass fiber sizings on selected mechanical properties of PET/glass composites. J. Adhes. Sci. Technol. 2000;14:651-60.

[8] Frenzel H, Mäder E. Influence of different interphases on the mechanical properties of fiber-reinforced polymers. Prog. Colloid Polym. Sci. 1996;101:199-202.

[9] Zinck P, Mäder E, Gerard JF. Role of silane coupling agent and polymeric film former for tailoring glass fiber sizings from tensile strength measurements. J. Mater. Sci.. 2001;36(21):5245-52.

[10] Ofir Y, Zenou N, Goykhman I, Yitzchaik S. Controlled amine functionality in self-assembled monolayers via the hidden amine route: chemical and electronic tunability. J. Phys. Chem. B. 2006;110(15):8002-9.

[11] Lee L-H. Wettability and conformation of reactive polysiloxanes. J. Colloid Interf. Sci. 1968;27(4):751-60.

[12] Bascom WD. Structure of silane adhesion promoter films on glass and metal surfaces. Macromolecules. 2002;5(6):792-8.

[13] Ishida H, Koenig JL. Fourier transform infrared spectroscopic study of the structure of silane coupling agent on E-glass fiber. J. Colloid Interf. Sci. 1978;64(3):565-76.

[14] Naviroj S, Culler SR, Koenig JL, Ishida H. Structure and adsorption characteristics of silane coupling agents on silica and E-glass fiber; dependence on pH. J. Colloid Interf. Sci. 1984;97(2):308-17.

[15] Wu S. Polymer interface and adhesion. The United States of America: Marcel Dekker Inc. 2001.

[16] Plonka R, Mäder E, Gao SL, Bellmann C, Dutschk V, Zhandarov S. Adhesion of epoxy/glass fibre composites influenced by aging effects on sizings. Compos. A: Appl. Sci. Manufact. 2004;35(10):1207-16.

[17] Wu HF, Dwight DW, Huff NT. Effects of silane coupling agents on the interphase and performance of glass-fiber-reinforced polymer composites. Compos. Sci. Technol. 1997;57(8):975-83.

[18] Gorowara RL, Kosik WE, McKnight SH, McCullough RL. Molecular characterization of

glass fiber surface coatings for thermosetting polymer matrix/glass fiber composites. Compos. A: Appl. Sci. Manufact. 2001;32(3-4):323-9.

[19] Cheng TH, Jones FR, Wang D. Effect of fibre conditioning on the interfacial shear strength of glass-fibre composites. Compos. Sci. Technol. 1993;48(1-4):89-96.

[20] Thomason JL. The interface region in glass fibre-reinforced epoxy resin composites: 3. Characterization of fibre surface coatings and the interphase. Composites. 1995;26:487-98.

[21] Liu XM, Thomason JL, Jones FR. XPS and AFM study of interaction of organosilane and sizing with E-glass fibre surface. J. Adhes. 2008;84(4):322-38.

[22] Mallarino S, Chailan JF, Vernet JL. Glass fibre sizing effect on dynamic mechanical properties of cyanate ester composites I. Single frequency investigations. Eur. Polym. J. 2005;41(8):1804-11.

[23] Ishida H, Koenig JL. An investigation of the coupling agent/matrix interface of fiberglass reinforced plastics by fourier transform infrared spectroscopy. J. Polym. Sci.: Polym. Phys. Ed. 1979;17(4):615-26.

[24] Wang D, Jones FR. Surface analytical study of the interaction between γ-amino propyl triethoxysilane and E-glass surface Part II: X-ray photoelectron spectroscopy. J. Mater. Sci. 1993;28(9):2481-8.

[25] Wang D, Jones FR, Denison P. Surface analytical study of the interaction between γ-amino propyl triethoxysilane and E-glass surface Part I: Time-of-flight secondary ion mass spectrometry. J. Mater. Sci. 1992;27(1):36-48.

[26] Roy R, Sarkar BK, Bose NR. Effects of moisture on the mechanical properties of glass fibre reinforced vinylester resin composites. Bull. Mater. Sci. 2001;24(1):87-94.

[27] Axelos MAV, Tchoubar D, Bottero JY. Small-angle X-ray scattering investigation of the silica/water interface: evolution of the structure with pH. Langmuir. 2002;5(5):1186-90.

[28] Yumitori S, Wang D, Jones FR. The role of sizing resins in carbon fibre-reinforced polyethersulfone (PES). Composites. 1994;25(7):698-705.

[29] Cheng TH, Zhang J, Yumitori S, Jones FR, Anderson CW. Sizing resin structure and interphase formation in carbon fibre composites. Composites. 1994;25(7):661-70.

[30] Basarir F, Yoon T-H. Preparation of γ-APS monolayer with complete coverage via contact printing. J. Colloid Interf. Sci. 2009;336(2):393-7.

[31] Mäder E, Pisanova E. Characterization and design of interphases in glass fiber reinforced polyproplyene. Polym. Compos. 2000;21(3):361-8.

[32] Demarquette NR, Moreira JC, Shimizu RN, Samara M, Kamal MR. Influence of temperature, molecular weight, and molecular weight dispersity on the surface tension of

polystyrene, polypropylene, and polyethylene. II. Theoretical. J. Appl. Polym. Sci. 2002;83(10):2201-12.

[33] Zhandarov S, Pisanova E, Mäder E, Nairn JA. Investigation of load transfer between the fiber and the matrix in pull-out tests with fibers having different diameters. J Adhes. Sci. Technol. 2001;15:205-22.

[34] Bayer T, Eichhorn KJ, Grundke K, Jacobasch HJ. FTIR spectroscopic studies of interfacial reactions between amino functionalized silicon surfaces and molten maleic anhydride copolymers. Macromol. Chem. Phys. 1999;200(4):852-7.

[35] Ishida H, Naviroj S, Tripathy SK, Fitzgerald JJ, Koenig JL. The structure of an aminosilane coupling agent in aqueous solutions and partially cured solids. J. Polym. Sci. Polym. Phys. Ed. 1982;20(4):701-18.

**Table captions**

Table 1. Surface properties and pull-out test results of fibre M1 as reference compared with them extracted either by toluene (T) or water (W)

Table 2: Absolute average surface compositions obtained from XPS investigation on M1 fibres

Table 3: Average C surface compositions and the degree of nitrogen protonation obtained from M1 fibres

**Figure captions**

Fig. 1. $^{1}$H NMR spectrum of acetone soluble part of PP dispersion and the peak assignment

Fig. 2. FTIR spectrum comparison of (a) wash-off of M1 fibre in water, (b) extraction of only γ-APS sized glass fibre in water, (c) acetone soluble part of PP dispersion, (d) wash-off of M1 fibre in toluene, (e) acetone insoluble part of PP dispersion, and (f) PP dispersion

Fig. 3: Tapping mode AFM surface topography images of glass fibres (a) M1 fibre, (b) M1-T fibre, and (c) M1-W fibre, the Z scale is 200 nm

Fig. 4. Zeta-potential as a function of pH for M1, M1-W, and M1-T fibres

**Tables**

Table 1. Surface properties and pull-out test results of fibre M1 as reference compared with them extracted either by toluene (T) or water (W)

| Fibre | wt. loss[1] (wt.%) | $\theta_a$[2] (deg) | $\theta_r$[3] (deg) | $\theta_a - \theta_r$ (deg) | $R_q$[4] (nm) | $R_{max}$[5] (nm) | $\tau_d$[6] (MPa) | $G_{ic}$[7] (J m$^{-2}$) | $\tau_{app}$[8] (MPa) |
|---|---|---|---|---|---|---|---|---|---|
| M1 | / | 94.3 | 68.5 | 25.8 | 3.5 | 41.5 | 13.1 | 5.5 | 8.2 |
| M1-T | 0.35 | 99.2 | 72.0 | 27.2 | 9.6 | 88.6 | 10.6 | 3.7 | 6.4 |
| M1-W | 0.48 | 74.4 | 39.6 | 34.8 | 4.6 | 59.2 | 21.0 | 14.6 | 9.4 |

[1]wt. loss: weight loss, [2] $\theta_a$: advancing contact angle, [3] $\theta_r$: receding contact angle, [4] $R_q$: root-mean-square roughness, [5] $R_{max}$: maximum height roughness, [6] $\tau_d$: local adhesion strength, [7] $G_{ic}$: critical interphase release rate, [8] $\tau_{app}$: apparent adhesion strength

Table 2: Absolute average surface compositions obtained from XPS investigation on M1 fibres

| Fibre | TOA (deg) | Information depth (nm) | Average surface composition (in at. %) | | | | | |
|---|---|---|---|---|---|---|---|---|
| | | | O | N | Ca | C | Si | Al |
| M1 | 90 | 8 | 18.1 | 1.5 | 1.3 | 71.2 | 5.9 | 2.0 |
| | 60 | | 14.9 | 1.2 | 0.9 | 74.3 | 4.7 | 4.0 |
| | 30 | | 10.7 | 1.1 | 0.6 | 80.7 | 3.7 | 3.2 |
| | 15 | 2-2.5 | 8.9 | 0.9 | 0.6 | 86.3 | 2.6 | 0.8 |
| M1-T | 90 | 8 | 20.6 | 1.5 | 1.9 | 66.6 | 7.5 | 1.8 |
| | 60 | | 17.7 | 1.4 | 1.5 | 72.2 | 6.1 | 1.3 |
| | 30 | | 11.9 | 1.4 | 1.0 | 79.6 | 5.1 | 1.0 |
| | 15 | 2-2.5 | 8.8 | 1.0 | 0.7 | 85.6 | 3.8 | 0.3 |
| M1-W | 90 | 8 | 24.8 | 0.9 | 1.4 | 60.0 | 11.1 | 1.9 |
| | 60 | | 24.2 | 0.8 | 1.2 | 61.5 | 10.3 | 2.0 |
| | 30 | | 21.2 | 0.9 | 0.8 | 64.6 | 10.6 | 1.9 |
| | 15 | 2-2.5 | 18.7 | 1.1 | 0.8 | 67.8 | 10.6 | 0.9 |

Table 3: Average C surface compositions and the degree of nitrogen protonation obtained from M1 fibres

| Fibre | TOA (deg) | C surface composition (in at.%) | | | | $N^+$ (in at.%) |
|---|---|---|---|---|---|---|
| | | C-1 | C-2 | C-3 | C-4 | |
| M1 | 90 | 73.2 | 20.7 | 4.3 | 1.8 | 10.5 |
| | 60 | 73.3 | 20.4 | 4.5 | 1.8 | 0 |
| | 30 | 74.9 | 18.5 | 4.9 | 1.7 | 0 |
| M1-T | 90 | 81.9 | 11.8 | 4.0 | 2.3 | 20.2 |
| | 60 | 79.2 | 14.1 | 4.2 | 2.6 | 25.2 |
| | 30 | 77.5 | 15.9 | 4.2 | 2.5 | 0 |
| M1-W | 90 | 79.6 | 14.4 | 3.8 | 2.2 | 48.4 |
| | 60 | 78.9 | 14.1 | 4.7 | 2.4 | 42.2 |
| | 30 | 79.1 | 14.3 | 4.3 | 2.3 | 35.1 |
| Binding energy (eV) | | 285.0 | 286.4-286.5 | 287.4-287.5 | 288.7-289.0 | |
| Chemical state | | C-C | C-N/C-O | C=O/O-C-O | C-O-(C=O)/$CO_3$ | |

**Figures**

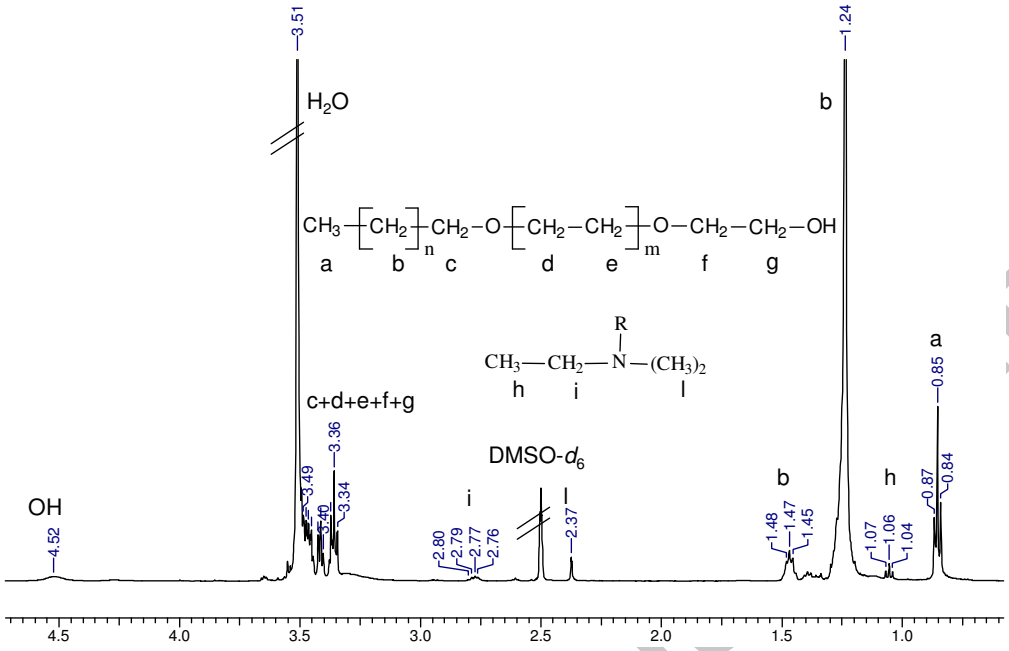


Fig. 1. $^{1}$H NMR spectrum of acetone soluble part of PP dispersion and the peak assignment

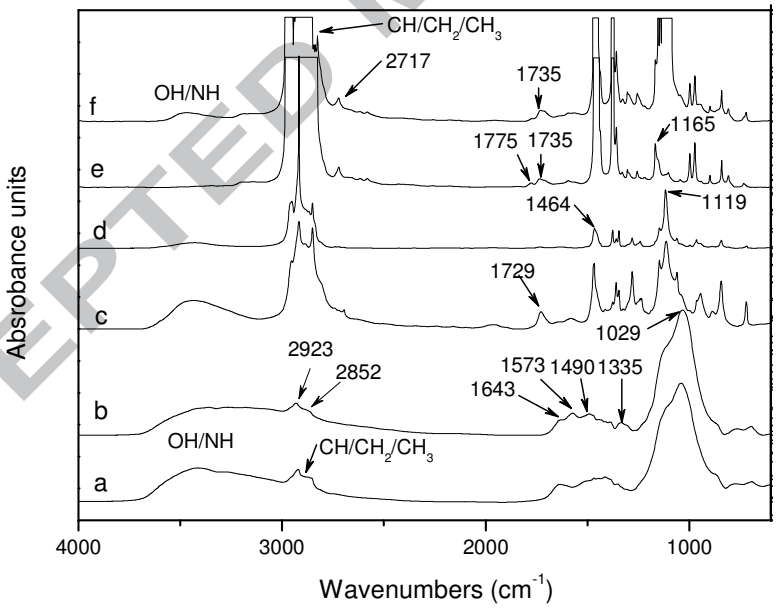


Fig. 2. FTIR spectrum comparison of (a) wash-off of M1 fibre in water, (b) extraction of only γ-APS sized glass fibre in water, (c) acetone soluble part of PP dispersion, (d) wash-off of M1 fibre in toluene, (e) acetone insoluble part of PP dispersion, and (f) PP dispersion

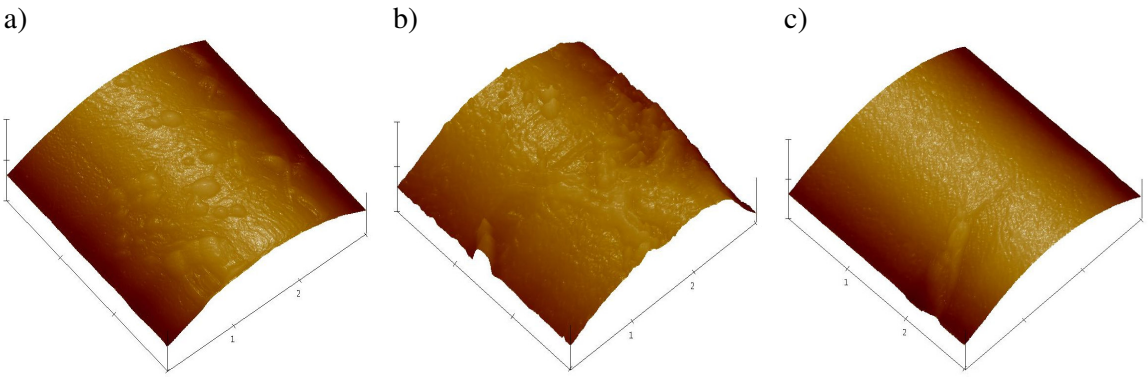


Fig. 3: Tapping mode AFM surface topography images of glass fibres (a) M1 fibre, (b) M1-T fibre, and (c) M1-W fibre, the Z scale is 200 nm

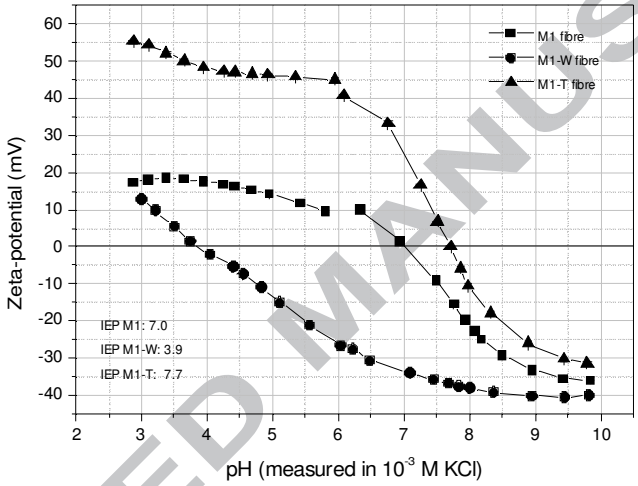


Fig. 4. Zeta-potential as a function of pH for M1, M1-W, and M1-T fibres